CrossMark

Three-dimensional reservoir architecture modeling by geostatistical techniques in BD block, Jinhu depression, northern Jiangsu Basin, China

Xue Li[1] · Jinliang Zhang[2] · Longlong Liu[2] · Zhongli Fan[3] · Guangxue Zhang[3] ·
Cunlei Li[3]

Abstract To reduce or avoid some of the ambiguities in a heterogeneous reservoir, a fine three-dimensional model would be inevitably established with the application of geostatistical techniques. BD oilfield is a low-permeability fractured reservoir with many fracture types, which composes a multi-azimuthal fracture system, causing strong anisotropy and heterogeneity. Moreover, fracture provides not only accumulation space for oil and gas but also channels for migration of hydrocarbons and water dashing and thus plays a leading role in controlling BD reservoir production. With the continuous exploitation of oil in reservoir for more than 30 years, BD oilfield has currently stepped into high water cut stage, exposing many problems such as low oil recovery, poor exploitation stability, rapid oil production decline, and one-way water intrusion. Therefore, a detailed reservoir characterization, constructed to describe reservoir behavior under strong water drive in a well-developed fractured reservoir, is urgently needed. In this study, combined with three-dimensional geostatistical techniques, an accurate and efficient reservoir parameter model that occurs in a strong heterogeneous fractured reservoir has been constructed through stratigraphic correlation and sedimentary facies analysis. Hence, all the study presented above will be available for well location, remaining oil potential-tapping and oil recovery improvement during the later study work.

Introduction

Three-dimensional modeling, which is used for predicting future performances or determining optimal locations of infill wells (Tureyen and Caers 2005), is an essential task in reservoir characterization study and also plays a crucial role in the efficient recovery of hydrocarbons initially in place (Kulpecz and van Geuns 1990), especially in complex fractured reservoirs. Geostatistical modeling and visualization require extension of traditional GIS methods (Turner 1989), and detailed definition of subsurface geology requires volumetric representation referenced to three orthogonal axes, rather than just topographical, formation environmental, hydrological, and areal extents of geological characteristics (Turner 2006). These volumetric data must be analyzed by computer-based 3D systems designed to handle the variety of geoscience data and geostatistical analysis need (Turner 2000). Hence, these reservoir models must be conditioned to all available data and various technologies in order to understand a prospective reservoir and provide information at many different scales accordingly (Al Bulushi et al. 2012; Chen and Durlofsky 2006). Three-dimensional modeling process is subdivided into the following three steps: data processing, actual 3D modeling, and visualization, respectively; however, in some cases, model reliability evaluation and further revision are included if reservoir heterogeneity and interval deposition difference cannot be well reflected or the established model cannot coincide well with the actual geology setting (Laine 2014),

✉ Xue Li
lix@cczu.edu.cn

1 School of Petroleum Engineering, Changzhou University, Changzhou 213016, China

2 College of Resources Science and Technology, Beijing Normal University, Beijing 100875, China

3 College of Geological Science and Engineering, Shandong University of Science and Technology, Qingdao 266500, China

🍂 Springer

which can be attributed to the following two aspects. On one hand, the reservoir characteristics depend on its geological background, thereby forming its unique sedimentary characteristics. On the other hand, under the influence of local structure and internal sedimentation, there exists a time (geological periods) and space (depositional environment) difference despite in the same period (Monsen et al. 2005). The main purposes of this paper are to present and define (1) the stratigraphic framework and 3D geological modeling of a multi-layered stratum to assess the distribution of subsurface geological sequences; (2) facilitate geological conceptualization and characterization, which will be used thereafter in the development of remaining oil recovery in the complex fractured-block reservoirs during high water cut stage; and (3) the production of cross sections and fence diagrams to visualize and analyze the spatial extension of geological properties and their geometric form.

Geological background

Northern Jiangsu Basin belongs to the land part of Northern Jiangsu-South Yellow Sea Basin. It is surrounded by Lusu uplift to the west, Sunan uplift to the south, South Yellow Sea Basin to the north, and Jianhu uplift to the northwest, respectively. The south of Jianhu uplift is Dongtai depression, and the north is Yanfu depression which consist of Gaoyou depression, Jinhu depression, Qintong depression, Hai'an depression, and Yancheng depression (Mao et al. 2006).

Northern Jiangsu Basin is composed by many small-scale dustpan sags. Its hydrocarbon pooling has the following characteristics: (1) the Late Eocene is the pooling period; (2) source rock is one-way hydrocarbon expulsion; and (3) the migration and accumulation styles are different in Eocene fault depression and Palaeocene depression. In the depression system, hydrocarbon migration pathway is in vertical direction due to unconnected sand bodies. Reservoirs, especially structural-lithologic oil-gas reservoirs, mostly distribute in deeper depression and range along the fault; (4) hydrocarbon accumulation is mainly controlled by sandstone property, fault sealing, and source rock maturity.

BD oilfield is located in Biantang village, Jinhu County, Jiangsu Province. It constructs on Minqiao-Biantang fault belt, the southern part of Jinhu depression, displaying a northward fault-nosing structure (Fig. 1). The upward stratigraphic sequence of BD oilfield is Funing Formation, which is composed by four members (including the first member E_1f_1, the second member E_1f_2, the third member E_1f_3, the fourth member E_1f_4 upward, respectively); the second member of Dainan Formation (E_2d_2), Sanduo Formation, which is composed by two members (including the first member E_2S_1, the second member

E_2S_2); and the second member of Yancheng Formation (N_2Y_2), Dongtai Formation, respectively. The third oil set of the second member of Funing Formation ($E_1f_2{}^3$) are the focus of this study (shown in Fig. 2).

Material and method

Through the whole process of modeling, the geological spatial information modeling is a crucially important technique combined with geoscience statistics, spatial prediction, and stochastic interpolation (Zheng and Shen 2004; Tao et al. n.d.). In this study, all samples were collected from 9 cored wells and other 50 wells whose depth mainly concentrate at $E_1f_2{}^3$. Petrographic observation which was performed by SEM is used to identify minerals, pore textures, and clastic composition. Besides, stochastic interpolation, which refers to the process of filling in unknown values in a sequence based on known values, was applied to the geological modeling of sparse spatial and structural data within a 3D digital environment. The shape being modeled was outlined by exploring the utility of using free-form surfaces to model geological data to ensure that surface features of varying frequency are well characterized. Constrained Discrete Smooth Interpolation (DSI) was conducted to improve the smoothness of regional control frame, which is used to extend beyond the original domain to include neighboring features or features at an extended regional scale (control scattered pieces of localized model data, resulting surfaces, etc.). In order to make accurate prediction as much as possible and thus achieve the goal of fine reservoir characterization accordingly, an overall borehole data fitting method was used to characterize geological spatial information by creating different stratum interface (Zhang et al. 2011). Two kinds of contouring methods, which rely on extracting isolines from regular 2D grid of interpolated values or from triangles created using automatic triangulation algorithms, were adopted to create constraint surfaces. During the process of building stratum surface, Automatic Surface Fitting (ASF) was conducted based on contouring of a set of Z values in an X-Y plane. According to verifying eight vacuating well parameters such as structure and sand body thickness that have been predicted by model, it showed high coincidence rate of more than 90 % to real datum. As for the property modeling, sequential indicator simulation and assigned value simulation were both applied; the former was more conducive to display reservoir heterogeneity, while the latter was a type of deterministic modeling method that can be used to construct mudstone model.

The up-to-date availability of high-performance techniques, including 2D and 3D interpolation and computer graphics, were used for data handling. Based on the

available information obtained about the reservoir, especially from well drilling and logging, three-dimensional geological model was established to (1) characterize

reservoir, (2) to further study restriction factors of reservoir development, and (3) to optimize the oilfield development adjustment plan.
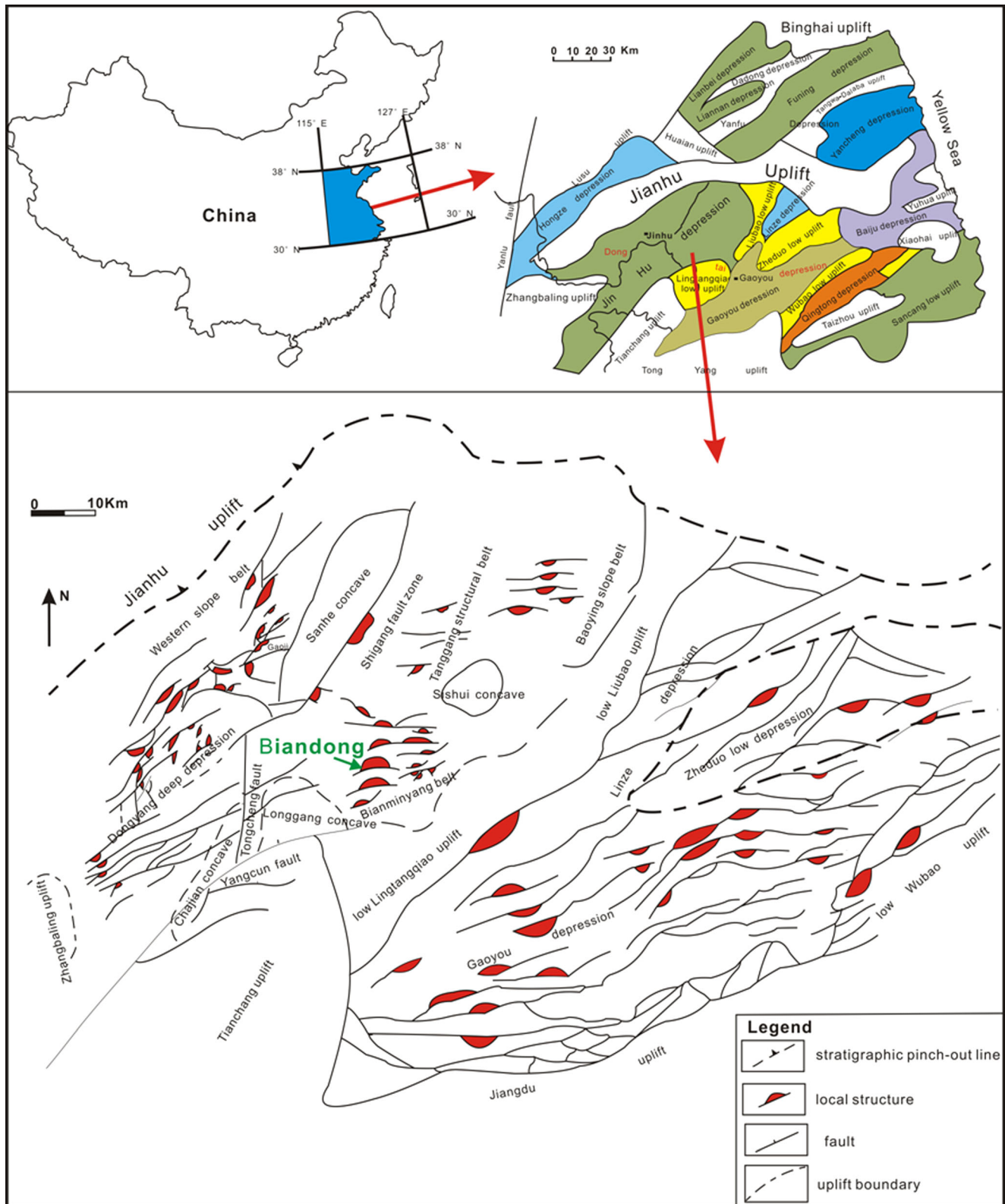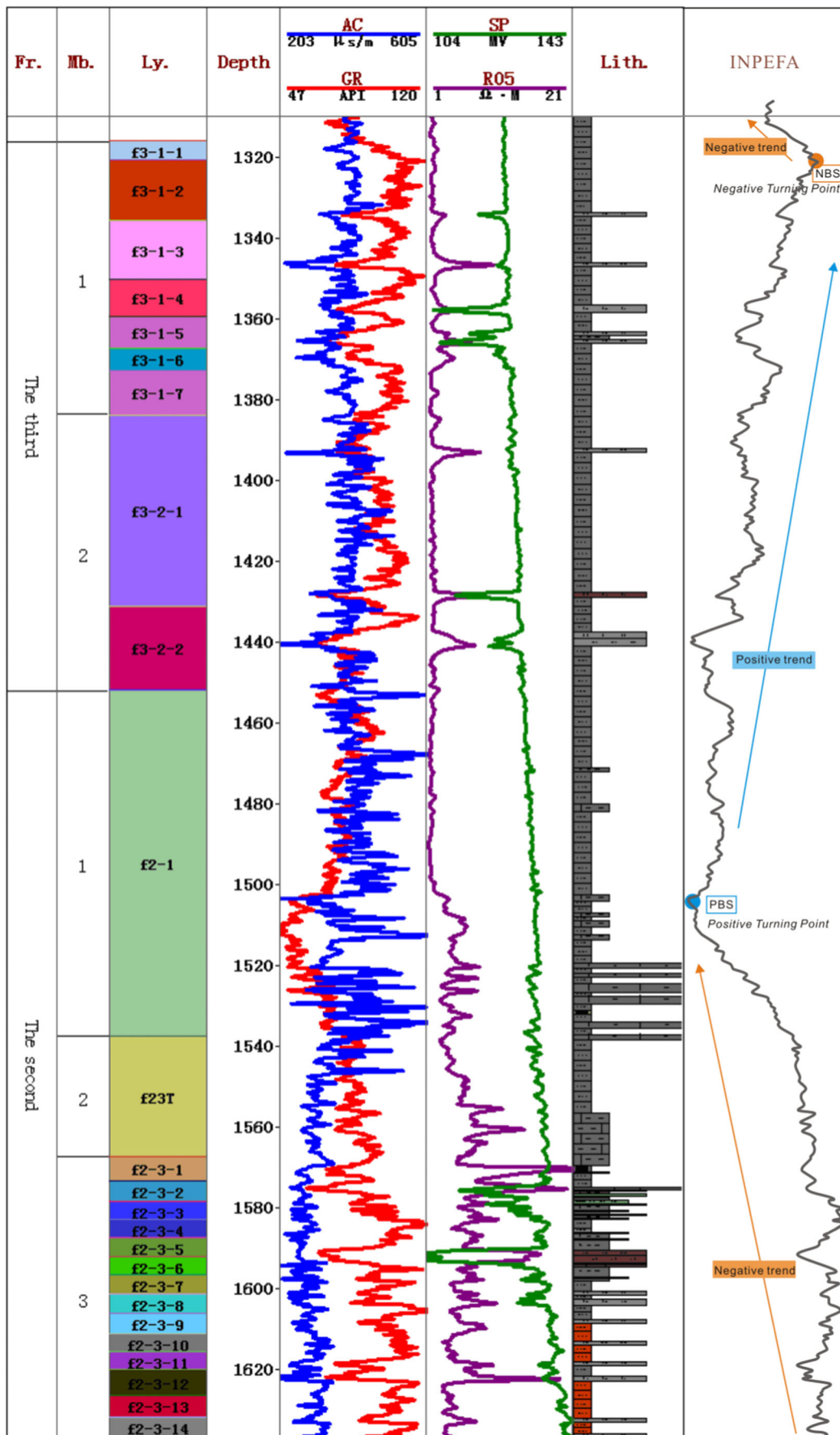

Fig. 1 The geological location map of the study area, BD oilfield is outlined by *green fonts*

Results and discussions

The primary goal of geological modeling is to identify the most significant vertical and lateral heterogeneities within the reservoir and incorporate this information into three-dimensional geologic models (Durlofsky et al. 1997). Considering the varied types of characteristics we need to describe, the type of available data has to come from a broad spectrum of sources (Tureyen and Caers 2005; Yeten and Gumrah 2000). These types of data mainly include geological descriptions, log and core data, drilling data, and seismic data.

Spreadsheets of digital borehole data from more than 50 wells are used, from which it can be obtained well drilling depth, inclination and azimuth, sand body configuration, sediment texture, and elevation of changes in textural characteristics recorded by the well drill.

Sedimentary environment and lithological characteristics

The color index is an intuitive reflection of physical and chemical conditions for sedimentary rocks during their formation period. The color value of the second and third members of Funing Formation ranges from −60 to −100, except small amounts of positive values in $E_1f_2^3$. Starting from the second member of Funing Formation (E_1f_2), all the values turned
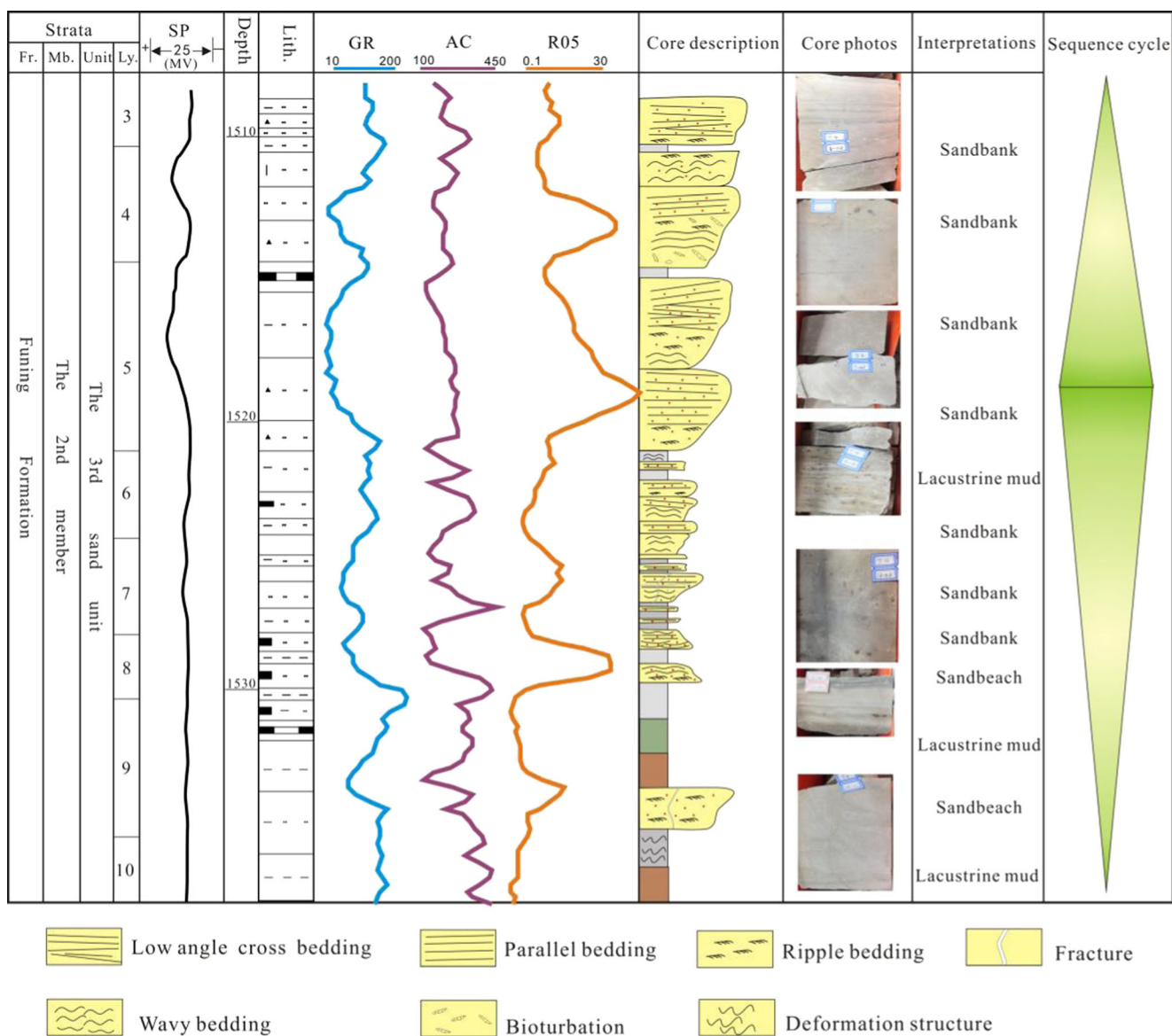

Fig. 3 Single well facies analysis and depositional sequence cycles of the third sand unit of the second member of the Funing Formation. *Fr* Formation, *Mb* member, *Ly* layer, *Lith* lithology

negative and keep increasing with depth, indicating that the sedimentary environment gradually change into reducing environment and water gradually deepening as well.

In the segment of E_1f_2, the dominant mudstone color is dark gray and gray-black; red or purple mudstone is relatively rare. Compared with the northwest of the study area, the color value is relatively higher in the southeast, then shows a trend of gradual decrease in color value to the north, gradually give priority to reduced color. These changes indicate that the shoreline is proximally in the direction of east by north. As to the third member of Funing Formation (E_1f_3), the mudstone color is similar to that of E_1f_2, dominated by dark gray and gray-black sandstones.

It develops a mixed deposition in $E_1f_2^3$ under the shallow lake environment. And, the mixed deposition can be subdivided into mixed sandbar, mixed sandbeach, and semi-deep lake; among these depositions, the dominated deposition of the study area are mixed sandbar and mixed sandbeach. The third member of Funing Formation (E_1f_3) develops a set of shallow water delta front deposition.

The coring interval of well B4 mainly concentrated in the third to the tenth layer, among of which the third to the fifth layer have the well-developed sand bodies, showing a typical coarsening upward sequence of sandbank deposition, with the main bedding of parallel bedding and ripple bedding combined with occasional bioturbation at the bottom of sand bodies. The fifth layer has the largest thickness of sand bodies with oil stains. The sand thickness shows a decreasing trend between the sixth layer and the eighth layer which is dominated by wavy bedding and an increasing thickness of shale content. In the seventh layer, it develops parallel and high-angle fractures with the width between 10 to 15 cm. At the bottom of the ninth layer, there is thin sandstone of 1-cm width and vertical fractures of 20-cm length within sand body. The main lithologies of upper ninth layer are gray-green and brown mudstone. At the top of the tenth layer, it develops gray sandy mudstone with internal deformation structure, and the bottom is brown mudstone. Sedimentary sequence of the second member of the Funing Formation in well B4 is shown in Fig. 3, displaying a vertical sedimentary section of the sandy beach bar deposition.

Reservoir property characteristics

Having experienced long-term evolution, the sedimentary sequence of BD has experienced different stages of diagenesis, forming huge thickness. The diagenetic stage of BD oilfield can be divided into early A stage, early B stage, and late A stage. Having undergone compaction, early carbonate filling, and recrystallization in early diagenesis stage A, reservoir porosity has been reduced to about 20 % at the depth of 1270 m. In early B stage, diagenesis is given priority to cementing, and primary porosity declined to about 15 %. As for late A stage, dissolution is the main diagenesis.

From the statistic analysis on thin sections of core samples, the conclusion is that the lithology of $E_1f_2^3$ is mainly lithic feldspathic sandstone, followed by feldspar lithic sandstone with small amounts of feldspar quartz sandstone and lithic quartz sandstone. Quartz account for 65 % of the clastic components and thus become the highest content, while feldspar and lithic account for small proportion. The compositional maturity of sandstone is relatively higher with an average of 2.16.

Table 1   Porosity and permeability characteristics of the third oil set of the second member of Funing Formation ($E_1f_2^3$)

Stratohorizon		Type of sand body	Core porosity (%)			Core permeability (mD)		
Stratum	Layer		Minimum	Maximum	Average	Minimum	Maximum	Average
The third oil set of the second member ($E_1f_2^3$)	$E_1f_2^{3-1}$	Sandbank, sandbench, shallow lake	6.16	28.31	19.45	2	144	27
	$E_1f_2^{3-2}$		7.68	24.22	18.2	4	83	14
	$E_1f_2^{3-3}$		4.67	28.13	20	3	165	29
	$E_1f_2^{3-4}$		8.72	27.66	18.35	2	116	25
	$E_1f_2^{3-5}$		5.08	25.99	18.73	1	130	36
	$E_1f_2^{3-6}$		7.16	28.15	17.04	4	255	5
	$E_1f_2^{3-7}$		3.89	29.31	18.82	4	386	26
	$E_1f_2^{3-8}$		10.38	28.23	19.14	1	274	24
	$E_1f_2^{3-9}$	Sandbench, shallow lake	15.37	23.21	19.05	6	64	2
	$E_1f_2^{3-10}$		14.23	24.76	18.99	5	69	1
	$E_1f_2^{3-11}$		11.29	27.76	21.13	2	233	16
	$E_1f_2^{3-12}$	Sandbank, sandbench, shallow lake	12.11	26.56	20.03	2	158	11
	$E_1f_2^{3-13}$		8.93	28.9	20.04	13	322	5
	$E_1f_2^{3-14}$		1.88	27.55	18.98	1	171	34

The sand bodies of Funing Formation include shallow delta sand body, sandy beach bar, mixed bench bar, and delta sand body with burial depth ranging between 1600 and 1900 m. The sand body of objective interval E_1f_2 mainly includes sandbank sand body, sandbench sand body, and shallow lake. Generally speaking, their properties are larger than those in the first member (E_1f_1) but lower than E_1f_3. In vertical, due to the coarser grain size and larger thickness and widespread of sand bodies, the reservoir property of the third oil set is relatively better than other oil sets. Porosity and permeability characteristic of $E_1f_2^3$ are shown in Table 1.

The 3D structural modeling

Grid design

Taking oilfield size, well spacing density, vertical sampling density of data points, the model size, and data volume size into consideration, the combination of subjective evaluation and the objective analysis is applied to make the following principles in determining grid size of geological model:
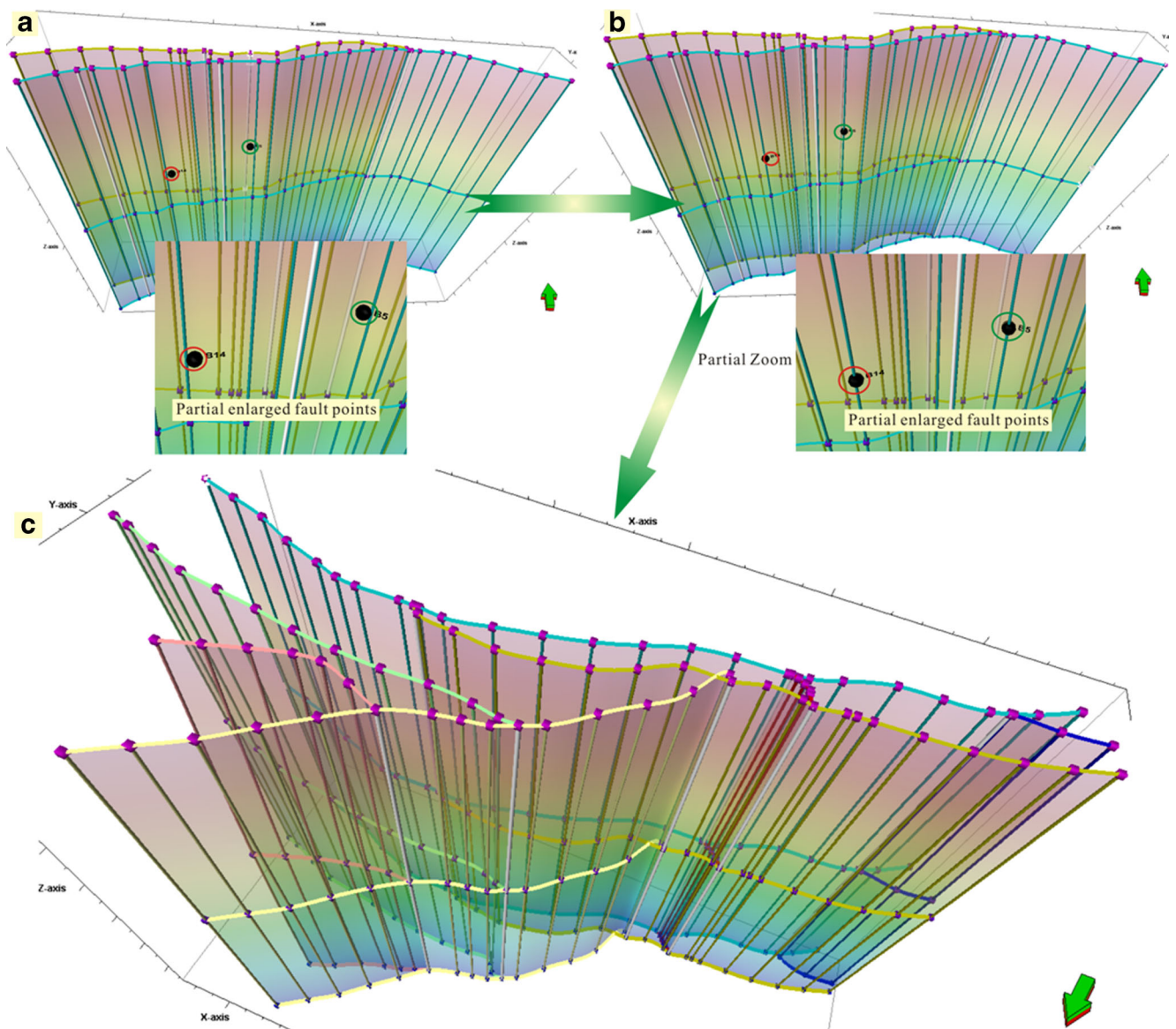
(1)   Isochronous modeling principles

Fig. 4 Three-dimensional fault model of the third submember of the second member of Funing Formation ($E1f_2^3$). **a** The initial fault plane, showing that some fault points are not on the fault plane; **b** adjustment of initial fault plane to ensure that fault plane and the break points are best matched; and **c** the final fault plane after repeated adjustments, showing the spatial distribution and spread of fault plane
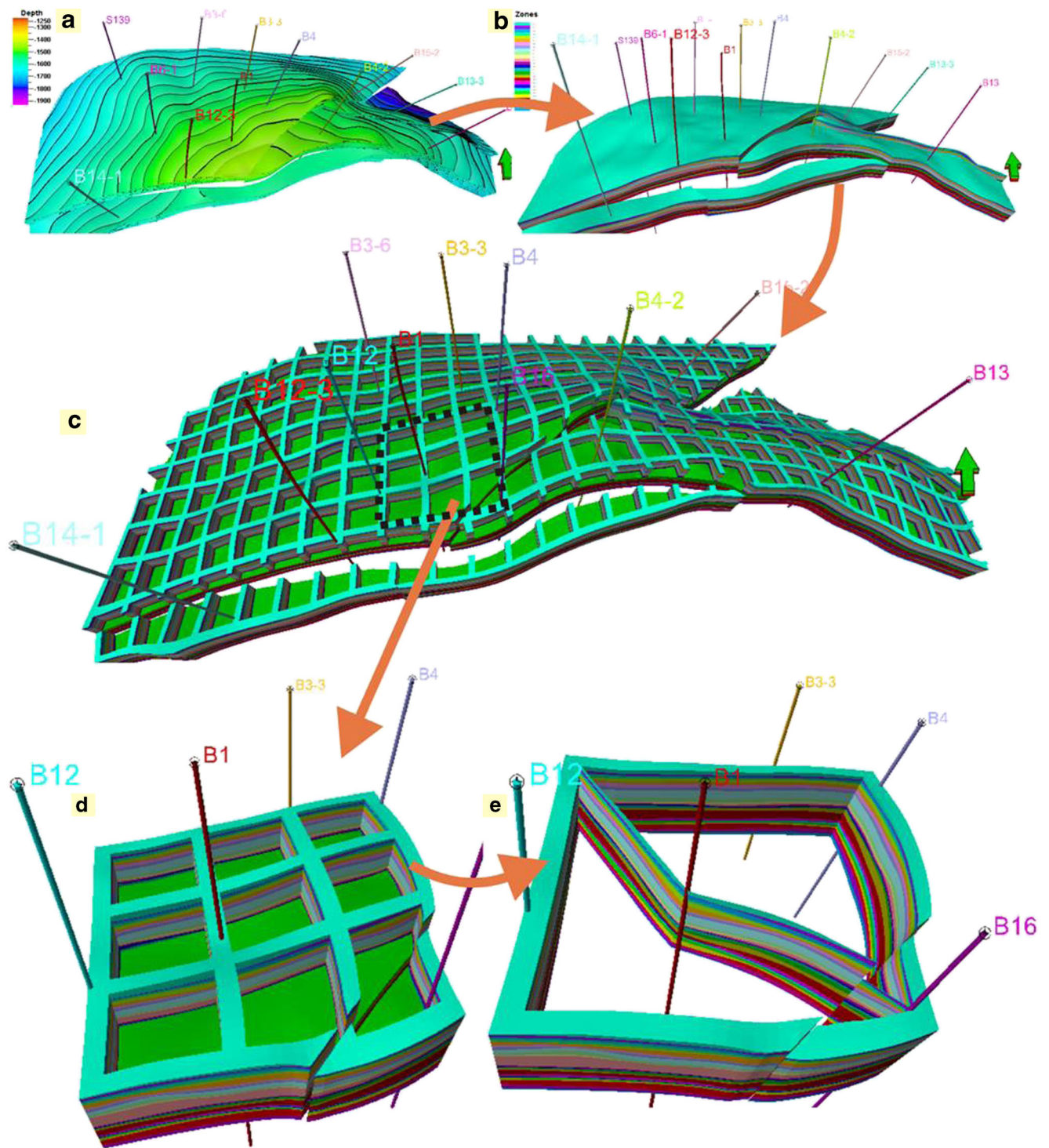
Fig. 5 Structural model of the study area, based on the horizon top structural interpretation analysis, integrating well top, and seismic data. **a** The 3D regional surface model, built with the constant control surface combined with interactive processing for stratum absence and reversion; **b** 3D regional structure model; **c** 3D through-well fence diagram of B at X axis (1, 2, 10), Y axis (1, 2, 10), and Z axis (16, 27, 5); **d** zoomed-in views of the *black boxes* in **c**, showing a detailed distribution pattern of internal structural model; and **e** through-well structural sections, showing the spatial stratigraphic distribution between wells in each layer

During the process of geological modeling, isochronous interface is utilized as geological constraints, and sedimentary bodies are thus divided into many isochronous layers according to isochronous modeling principles. Then, these isochronous layers are incorporated into a three-dimensional model of the entire reservoir.

(2) Integrated use of deterministic modeling and stochastic modeling

With the utilization of smoothing algorithm, the well-known data is smoothed to establish the reservoir model on condition that geological data is relatively abundant. To some degree, deterministic model, as the best depression of reservoir, comprehensively reflect the geology bodies. However, this method only takes into account the relevance of known well data except the unknown well data; thus, reservoir heterogeneity cannot be reflected accurately. On the contrary, based on random interpolation, stochastic modeling takes the relevance of all well data into consideration and generates serials of equal probabilistic models, which can also be viewed as the adjustment of the deterministic modeling with certain disturbance. During the actual modeling process, we can only do the best we can to combine stochastic modeling and deterministic modeling as much as possible; to minimize uncertainty of random interpolation, hence the modeling accuracy is improved; and so as to achieve reasonable reservoir heterogeneity description.

(3) Facies-controlled modeling

Sedimentary facies control the spatial distribution of sand bodies, and thus decide the reservoir parameters, so sedimentary facies modeling precedes the property modeling. Since the reservoir property varies on sedimentary facies, property modeling is constructed depending on facies belt (sand body types or flow units) through inter-well stochastic interpolation, and reservoir property model is obtained accordingly.

Modeling programs

(1) Establishment of modeling database
    The modeling database includes core test data, well-logging interpretation, drilling data, and well test data in types of coordinate data, logging data, hierarchical data, and reservoir characteristic data. These data are integrated to form a unified database for modeling. However, the quality of the original data is inevitably affected by the measuring instruments, data sources, or anthropogenic factors; QA is thus necessary for data from different sources to improve the accuracy of the modeling data.
(2) Establishment of qualitative geological model
    Based on the raw data and geological data, the qualitative geological model was established to provide guidance for selecting the preferred model.
(3) Determination of the characteristic parameters of the analog input
    Characteristic parameters include the statistical characteristic parameters and condition characteristic parameters.

(4) Stochastic simulation
    Based on the theory of stochastic function, multiple probability models are achieved with the method of stochastic interpolation.
(5) Model optimization and results

The quality of input data, modeling procedure, and the outcome values are all important for geological modeling, but there exists uncertainties at several levels within the model. Therefore, it is important to first assess the plausibility of each realization by checking the results of each modeling step against the conceptual geological model (Seifert and Jensen 1999). Finally, a set of model which mostly accord with the actual situation of reservoir characteristics is chosen from multiple probability models.

Among the five modeling steps, there is no strict order between the middle three parts, thus can be done alternately. Actually, geological modeling is a progressive realization process that proceeds from single well model, structure model, sedimentary microfacies model, and property model, respectively. Through the selection of the most appropriate simulation method according to the actual situation and geological data of the study area, the simulation process is made simple

Table 2 Main microfacies with their corresponding lithology, bedding structure, and pore of $E_1f_2^3$ in BD oilfield

Sedimentary pattern	Microfacies type	Lithology	Bedding structure	Pore type
Sandy bar deposition	Sandbar	Siltstone; argillaceous siltstone; oil-filled siltstone	Cross-bedding; parallel bedding; ripple bedding; wave bedding; oblique-bedding	Micropore; inter-grain pores; dissolved inter-grain pores; fracture
	Sandbeach	Oil-bearing fine-grained sandstone; cementing siltstone	ripple bedding; wavy bedding; parallel bedding	Micropore; few moldic pores; intercrystal pores; fracture
	Shallow lake	Mud rock and sandstone interbedded; gray green mudstone; brown mudstone	Wavy bedding; bioturbation structure	Rare pores

and optimal. Based on parameter adjustment and repeated modifications, the modeling work is completely finished.

Modeling methods

In all the modeling modules, reservoir property modeling which is obtained by inter-well property prediction is the core of geological modeling. Currently, the main modeling methods mainly include deterministic modeling and stochastic modeling (Archer and Wall 1992). Deterministic modeling, starting inference from known deterministic control point data (well point), gives deterministic predictions to unknown area, but this method bears the disadvantage that reservoir heterogeneity degree (discrete) is covered up, especially permeability heterogeneity, thus not suitable for characterizing permeability heterogeneity. Stochastic modeling is to give multiple equal probability of optional geological models to unknown area with the use of stochastic simulation methods, giving inter-well unknown region through random interpolation from known wells. Quantitative reservoir characterization can be realized, and also, heterogeneities in different scales can be characterized by stochastic reservoir modeling; therefore, stochastic modeling is increasingly becoming a significant trend in reservoir modeling.

Structural model

Structural modeling is practically a process of establishing the reservoir skeleton structure or the 3D reservoir grid, which starts with fault modeling. Fault, a kind of extensive geological structure, varies greatly depending on fault size; thus, different levels of fault exert different geological influences. A large fault controls regional geological structure and tectonic evolution, exerting the most control on the mineralization. While, medium and small faults control mineral deposit and the occurrence of the ore bodies as well. Different faults display different spatial fault plane pattern. In reservoir modeling, according to the flat shape of fault plane, faults can be subdivided into vertical fault, linear fault, listric fault, and curved fault, respectively (Zhao and Zhu 2001). Faults in different types require different amount of geological data and different characterization techniques as well.

According to the top structure map of E_1f_2, fault polygons are digitized and assigned, followed by an initial fault column and fault plane which is established with the use of pillar gridding. It is essential to smooth the initial fault plane repeatedly by adjusting fault location and its occurrence through single well stratigraphic correlation, to determine the location and depth of fault until the fault plane and break point are consistent (Fig. 4a, b), and also to ensure that the fault footwall

and tectonic surface are well matched (Fig. 4c). Compared to break point correlation, stratigraphic correlation is relatively easier. In this study, stratigraphic correlation was employed to adjust the fault plane. There are seven faults in total, and all the faults are in intersecting relationship. Among these faults, the southernmost fault was used as the boundary for geological modeling, and a best fit regional model is finally established with the application of fault truncation under the control of fault morphology and fault displacement.

Surface model, a three-dimensional visualization of stratigraphic interfaces fluctuation, is built based on fault model. The main principles we followed are as follows: (1) as to the place with well control, outliers were removed to keep strict accordance with the well data to ensure the accuracy of the structural form of the well region. (2) In the place without well control, the well tops of adjacent wells were used to control the surface trend. While in the case of few wells near the boundary of studied area, the regional structural map was used as the main reference, combined with human interaction technology to adjust hierarchical point, which did not coincide with surface, so as to improve the fitness between hierarchical points and surface if possible. (3) For the formation of the boundary faults, abnormal hierarchical points were adjusted according to the fault throw and the fault strike, dip, and other parameters, in the absence of well control.

There are totally 25 sand layers in the third submember of the second member of Funing Formation. In order to improve model precision, a constraint surface obtained by digitizing top structure map is used to establish the surface model of each layer; then, a regional surface model, composed by 50 layer (including sand layer and interlayer), is formed through the special superposition of layer model (Fig. 5a). Surface model is just an objective reflection of interfaces between layers, not real geological entities. And, the three-dimensional geological bodies of BD oilfield, filled between adjacent layers, were generated through the Geometric Modeling, shown as Fig. 5b. And, 3D fence diagram was consequently obtained to depict the internal features in detail (Fig. 5c–e).

Fig. 6 Sedimentary microfacies model of the study area, established ▶ with comprehensive application of sequential indicator simulation and interactive processing. **a** Vertical sedimentary sequence of single well, showing the types and depths of sedimentary microfacies zone. **b** Regression analysis of sand body thickness and width, providing guidance for the analysis of variation. **c** Variation analysis for each sedimentary microfacies except mudstone. **d** Regional sedimentary microfacies model. **e** Regional sedimentary microfacies model regardless of the fault by toggling simbox view
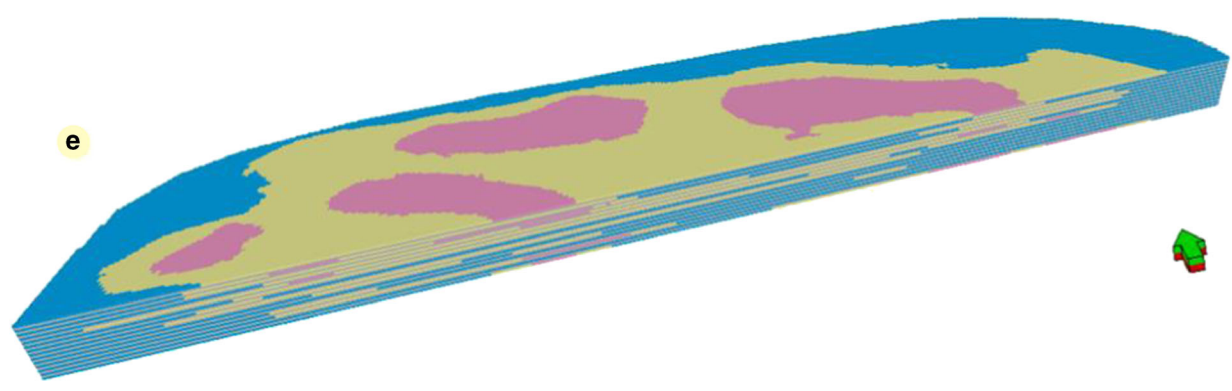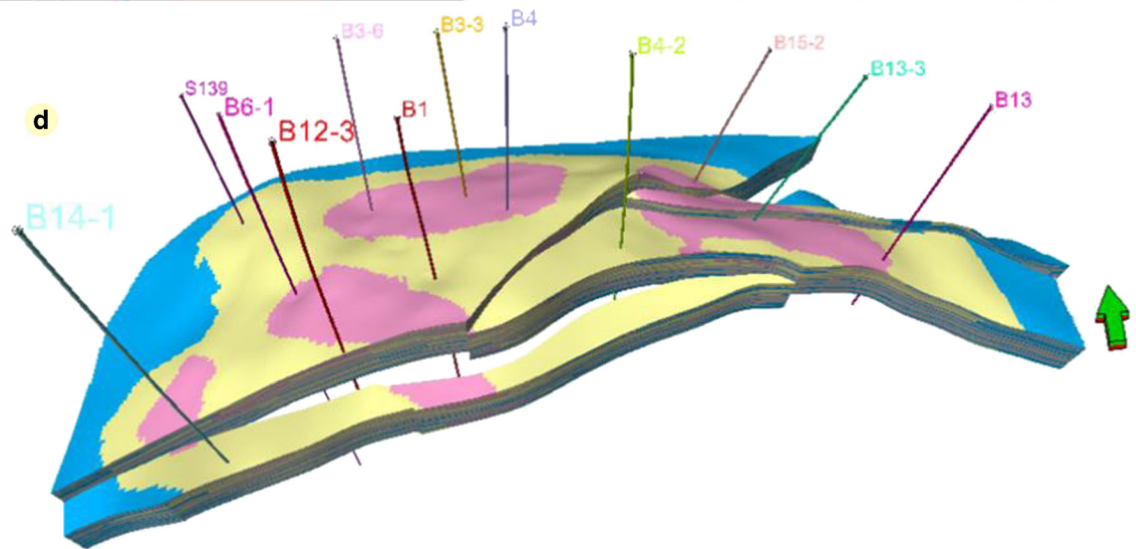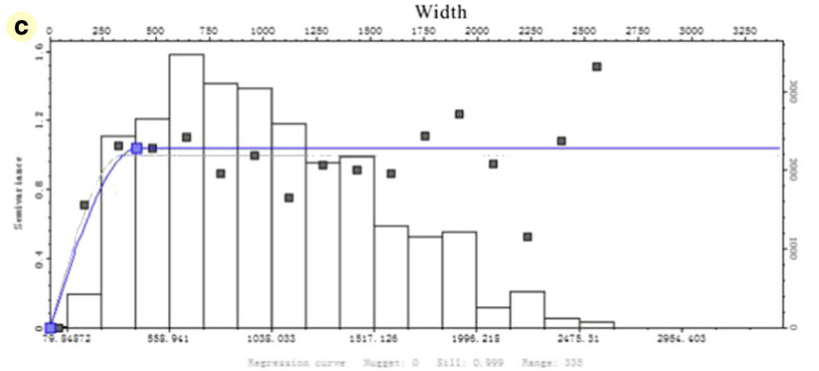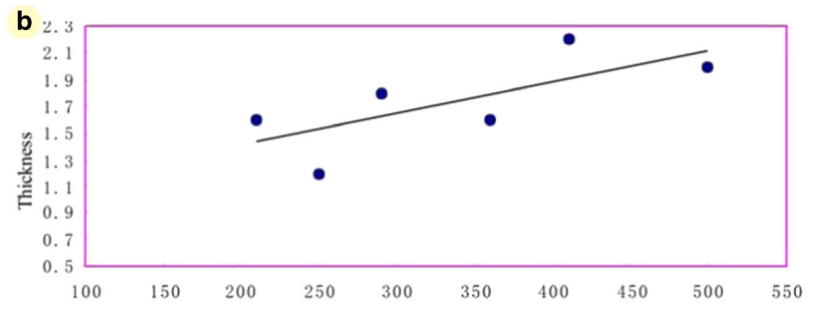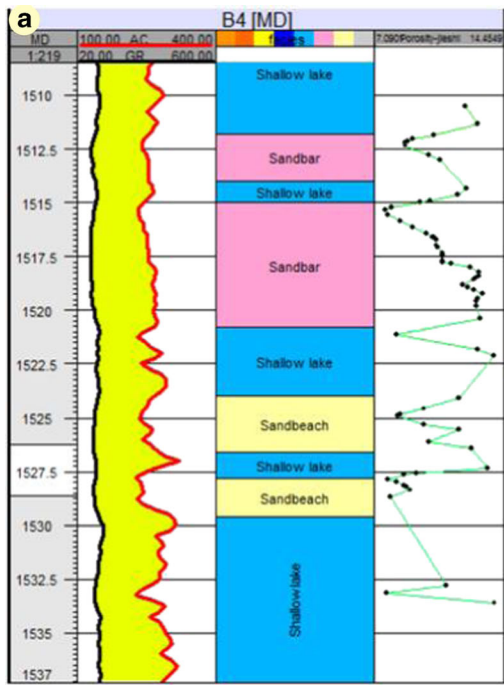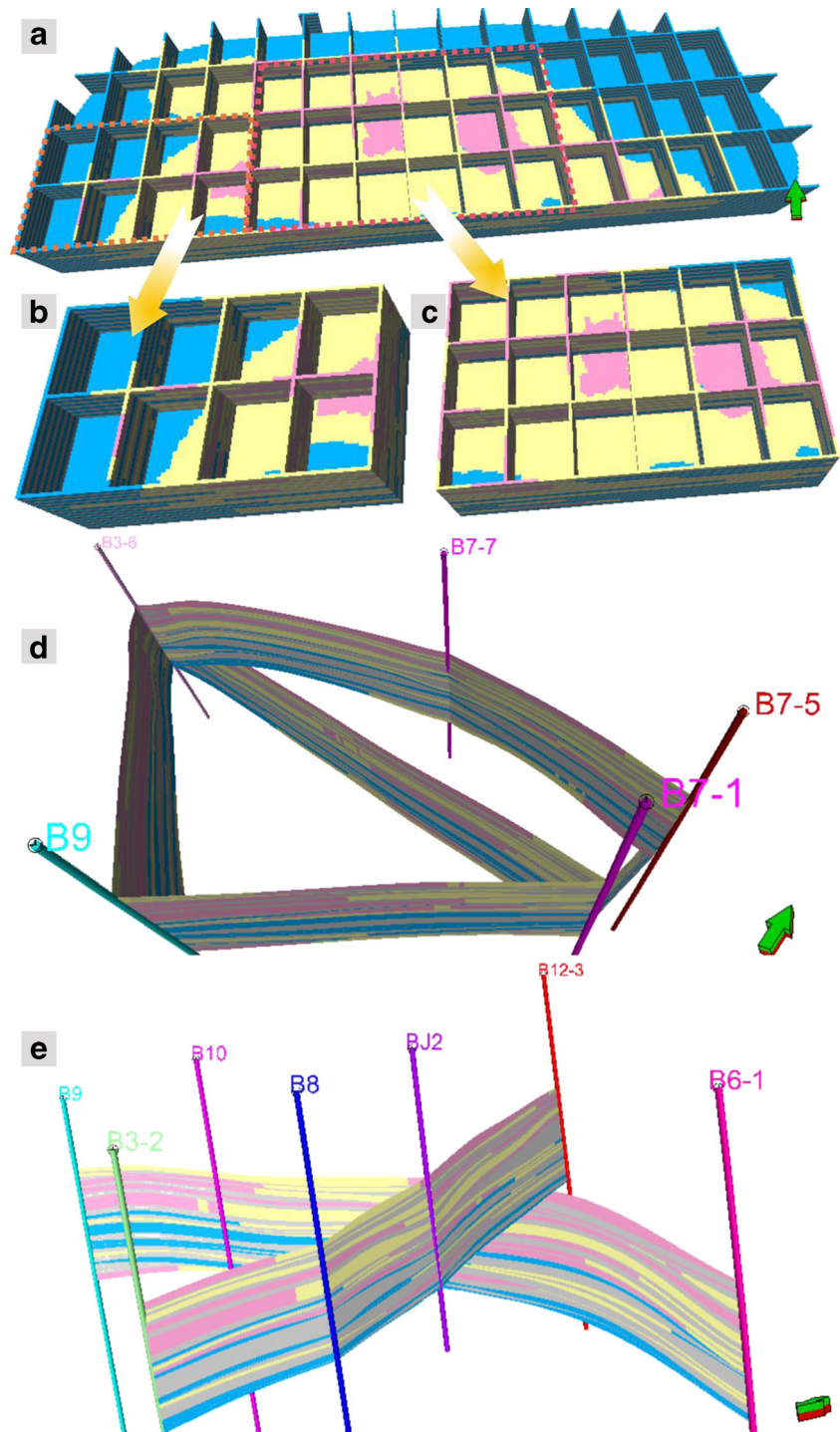
Sedimentary microfacies modeling

In order to improve the quality and efficiency of facies modeling, microfacies-transforming template was primarily established by segmenting the continuous logs into discrete zones with similar properties, which are the basic units of reference for inferring the correlation between wells (Wang et al. 2015). Microfacies are identified from sediment deposition environment through core observation of the visible features of rocks (Bhatt and Helle 2002); however, log facies is

Fig. 7 The 3D profile maps of sedimentary microfacies of the third submember of the second member of Funing Formation. **a** The 3D fence diagram of Fig. 6e at *X* axis (6, 1, 20), *Y* axis (6, 1, 26), and *Z* axis (13, 27, 5), regardless of the fault by toggling simbox view. **b**, **c** Zoomed-in views of the two *black boxes* in **a**, showing a detailed spatial distribution of microfacies model. **d**, **e** Connecting-well section of sedimentary microfacies model, showing the spatial distribution between wells in each layer

the response between lithology and logging curve. Thus, sedimentary facies can be reflected by logging facies. The focus of sedimentary microfacies identification is to extract logging characteristics to differentiate each microfacies when the data space is transformed into a feature space (Haykin 1999).

To carry out microfacies modeling, the most important step is the variogram analysis. Considering the relationship between provenance and physical distribution, variogram analysis was made in the following three directions: major, minor, and vertical directions, respectively. According to the orientation, the position, the width, the length, and longitudinal thickness of sedimentary units, the search coverage and band width of major and minor variograms were defined, so that the sample points are consistent with the theoretical variation function curve as far as possible.

According to the characteristics of reservoir sedimentary facies, comparison was implemented between truncated Gaussian simulation and sequential indicator simulation to choose suitable simulation method that can be used in facies modeling. There exists obvious transition boundary between two types of sedimentary facies in sedimentary facies model established with truncated Gaussian simulation; however, this kind of phenomenon does not appear in sedimentary facies model established with sequential indicator simulation. The transition between different sedimentary facies is more natural and thus more consistent with the actual geological characteristics. Sedimentary pattern of $E_1f_2^3$ is sandy bar deposition, and microfacies type include sandbar, sandbeach, and shallow lake, which can be reflected from lithology, bedding structure, and pore type (Table 2). Regional mocrofacies model was established with comprehensive application of sequential indicator simulation and interactive processing through variogram analysis and regression between sand body thickness and width (Fig. 6), and spatial profile of microfacies

model was consequently achieved in order to display a detailed spatial distribution of microfacies model between wells (Fig. 7), providing reliable basis for defining reservoir parameters of property modeling.

The 3D property modeling

Petrophysical parameter, the key elements of property modeling, has a significant influence on exploration and production studies for oil and gas industries (Fegh et al. 2013). The precise property parameters are obtained by laboratory measurement and well test interpretation. In this study, permeability is calculated by porosity-permeability formula, which is generated through linear regression of core porosity and permeability data (James et al. 2003). And, porosity is estimated using porosity-acoustic transforms obtained by linear regression of core porosity data and acoustic. Although there are many techniques used in modeling, geostatistics to reservoir modeling has solved the problem of data integration, model reliability, taken at different scales, into a more accurate reservoir numerical model (Wenlong et al. 1992). The primary aim of the study is to generate a regional model to reflect special inter-well heterogeneity associated with each reservoir property through the application of geostatistics.

Data analysis

Through the regression between acoustic and core porosity, combined with appropriate parameter adjustment, the reservoir porosity formula is achieved (Fig. 8a). Once the porosity formula is defined, the porosity-permeability formula will be achieved through the regression between porosity and permeability. Thus, the reservoir property value for each well is calculated accordingly (Fig. 8b). The reservoir porosity of
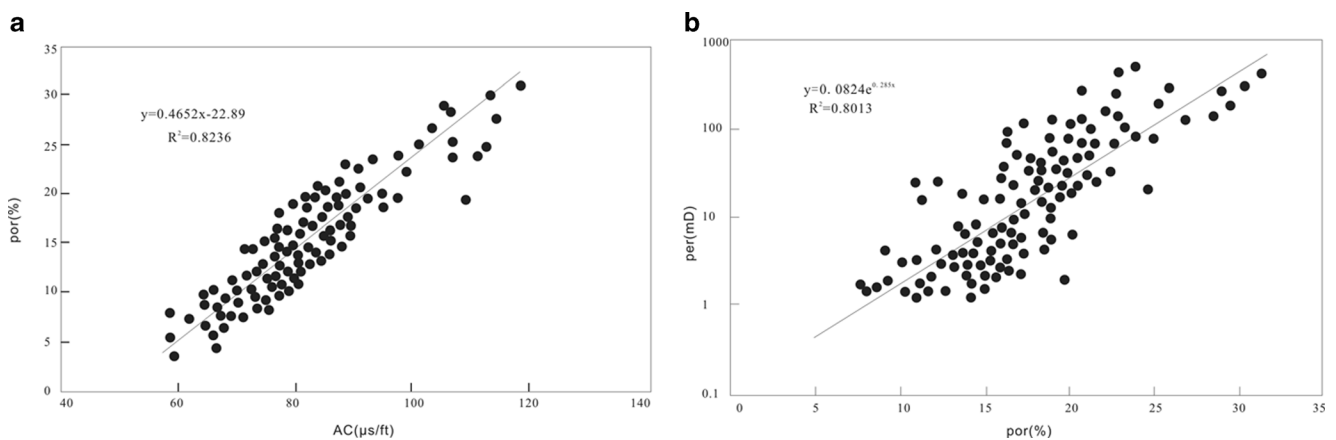

Fig. 8 The reservoir property formula of the study area. **a** The acoustic-porosity formula through regression between acoustic and porosity. **b** The porosity-permeability formula through regression between porosity and permeability

Fig. 9 Data processing for original property data to ensure a normal distribution. **a** The original input data of porosity (*left*) and the final data after output truncation (*right*). **b** The original input data of permeability (*left*) and the final data after output truncation (*right*)
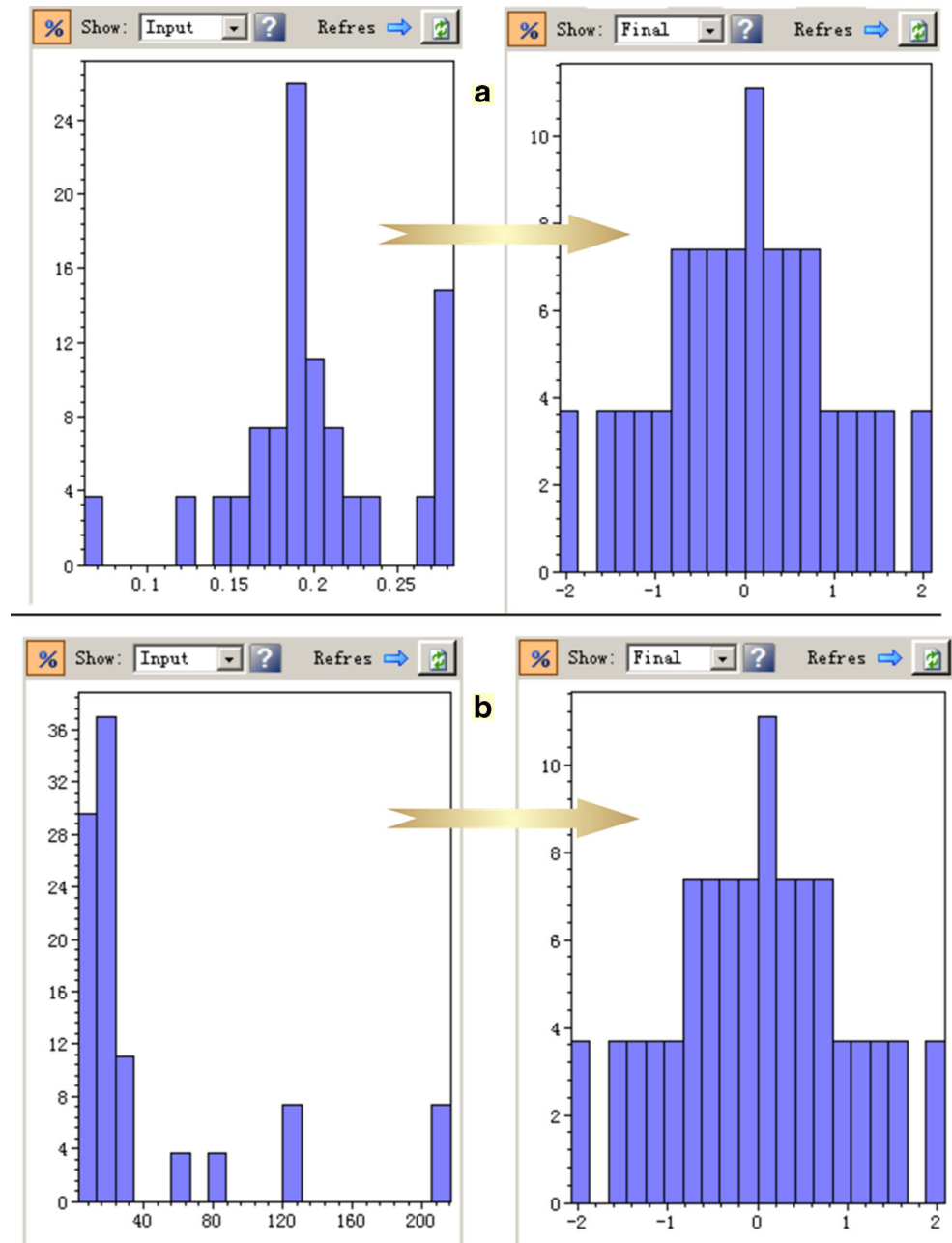
E_1f_2 distributes between 15 and 21 %, with an average of 17.6 %, and the permeability ranges between 5×10^{-3} and 100×10^{-3} μm^2 and 45×10^{-3} μm^2 on average. In contrast, the reservoir property of E_1f_3 is relatively better. Porosity shows a distribution area of 18 to 30 %, and permeability has an interval of 10×10^{-3} to 500×10^{-3} μm^2. According to the division criterion of clastic rock reservoir, E_1f_2 is a kind of reservoir with medium porosity and low permeability, while E_1f_3 has the characteristic of medium porosity and medium permeability. Porosity and permeability, as the two main reservoir parameters, depict the spatial distribution and planar distribution of reservoir property. Hence, the reservoir property models are mainly composed by permeability and porosity model. After comprehensive analysis of reservoir characteristics of BD oilfield, the main conclusion we come to is that an integrated use of sequential Gaussian simulation and Gaussian model is applied for porosity modeling, meanwhile sequential Gaussian simulation and exponential model is suitable for permeability modeling.

Data discretization of well-logging curve

Well-logging discretization is aimed to achieve longitudinal discrete data, which is also a process of making assignment to

Table 3 Variogram parameters for reservoir property simulation in sandbar sedimentary facies belt, a case of $E_1f_2^{3-1}$

Directional variogram Parameter	Major direction	Minor direction	Vertical direction
Number of lags	20	20	20
Lag distance	3500	2500	100
Lag tolerance	43.5	38.4	28.7
Bandwidth	1200	850	75

well-through grid cell. Thus, these assigned grid cell, which is a part of the property model, will be employed as constraints in the process of property modeling.

Since the resolution of well logs is higher than that of grid cell, it often causes one or more values in the same grid cell. However, in actual modeling process, we should adhere to the principle that the same grid cell allows only one value; thus, well logging should be discretized. There are mainly nine types of logging data discretization; they are arithmetic, harmonic, geometric, RMS, medium, minimum, maximum, midpoint pick, and random pick, respectively. Through making contrast of data distribution before and after data processing with these nine methods, it demonstrates that maximum algorithm is relatively suitable for discretization of reservoir property data to model permeability which mainly consist of porosity, permeability, and oil saturation.

Variogram analysis

Variogram, a tool used to characterize spatial changes on reservoir property, can quantitatively describe spatial correlation of regional variables. Its principle is that the closer the distance in space, the stronger the correlation will be. With the increase of the distance between the measured value, the similarity between the two measurements decreases (Isaaks and Srivastava 1989). However, when the distance exceeds a certain distance required by the minimum correlation, it will have no effect on spatial correlation. Experimental variance function formula can be expressed in the following:

$$\gamma^*(h) = \frac{1}{2N(h)} \sum_{i=1}^{N(h)} [Z(x_i) - Z(x_i + h)]^2 \qquad (1)$$

where h is the lag distance, $\gamma^*(h)$ is the variogram value at h, $N(h)$ is the number of lag distances, and $Z(x_i)$ is the value of the observation at point x_i (Deutsch 2002).

Since the correlation is anisotropic in space, we need to describe variogram function from different directions. Variogram function, obtained from input data, is used for property modeling, and spatial correlation of the experimental data can be reflected from the final model. The theoretical models of variogram function can be divided into the following four types: spherical model, exponential model, Gaussian

model, and power function model, respectively. And among all these models, the spherical model and the exponential model have high frequency of use in geological modeling.

Reservoir property model

The original data for property modeling is obtained by discretizing property data, which is calculated from physical formula. Due to the parameter distribution varying in depth and sedimentary zones, it will cause occasional inconsistent with the actual reservoir characteristics. Therefore, at the beginning of property modeling, data analysis and filter is an essential implementation in advance and to ensure reasonable range of property data in each sedimentary zone.

The original data must be processed through input, output, and normal transforms, respectively, to ensure that data is in normal distribution (Fig. 9), thus to meet the requirement of Gaussian simulation. Compared with porosity, the range of permeability variation is relatively larger. In order to facilitate the establishment and improve accuracy of permeability model, normal transforms must be conducted before logarithmic transformation. Considering the analysis quality of variogram function (Table 3), it requires comprehensive understanding of the studied area combined with abundant modeling experience to improve the modeling accuracy and reduce the inaccuracy to the minimum. In Table 3, nugget and sill both use the default value of 0 and 1, respectively.

After logging data discretization and variogram function analysis, three-dimensional porosity and permeability models were generated using sequential Gaussian simulation (SGS) (Fig. 10a, d). Through-well profiles and fence diagram were made to depict spatial variation of the porosity and permeability distribution (Fig. 10b, c, e, f).

Model validation

In order to ensure the accuracy of reservoir property model and hence achieve an exact description of reservoir heterogeneity, it is required to make model quality assessment in several ways as follows:

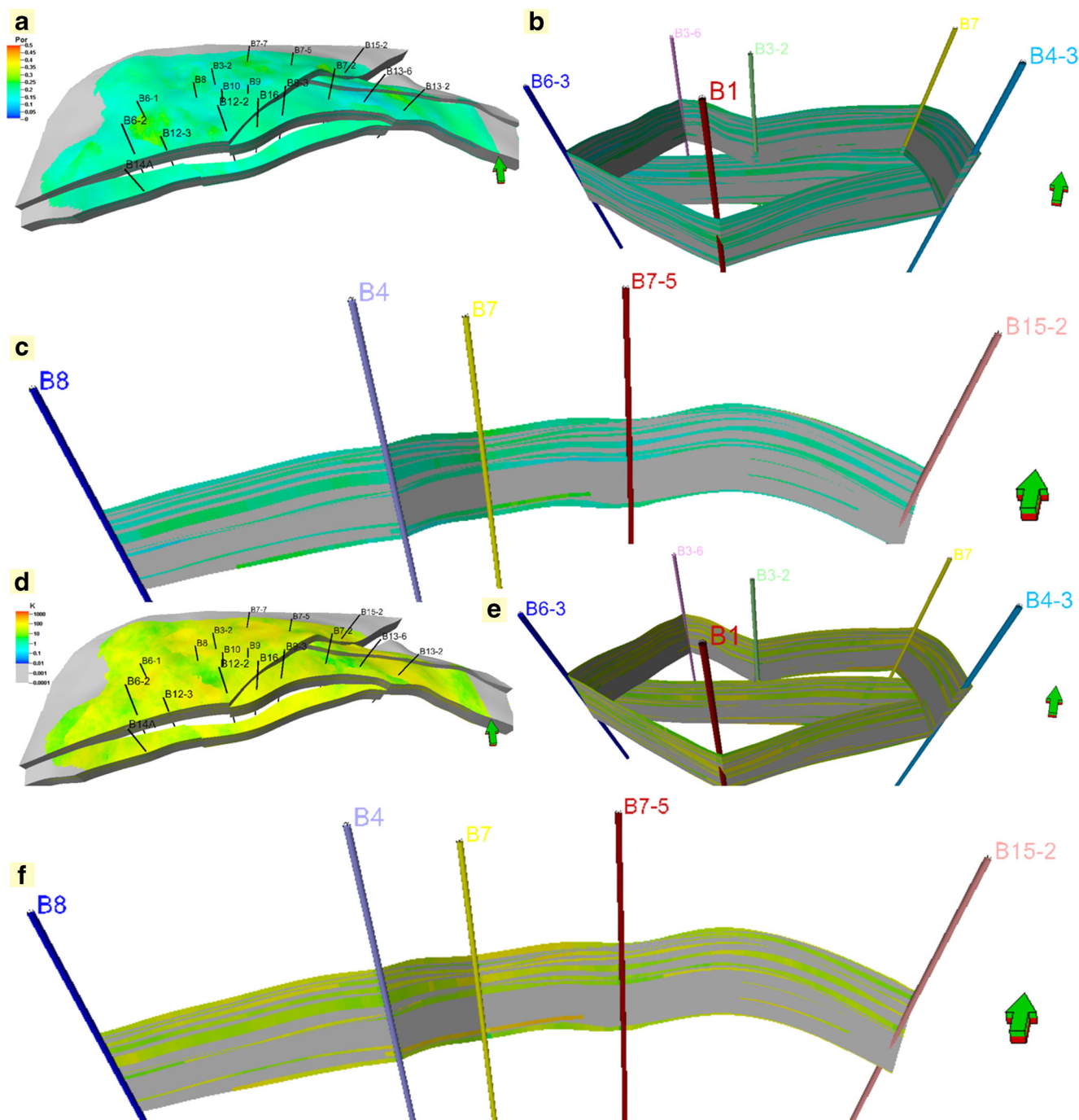(1) Modeling results coincide with the actual property characteristics of the reservoir

Fig. 10 The 3D profile maps of reservoir property of the third oil set of the second member of Funing Formation ($E_1f_2{}^3$) with sequential Gaussian algorithm for simulation mudstone facies and assigned values for mud facies. **a** The 3D regional porosity model established with spherical type. **b** The 3D fence diagram of A for well group B6–3~B1~B4–3~B7~B3–2~B3–6. **c** Connecting-well section of porosity model of B8~B4~B7~B7–5~B15–2, displaying spatial porosity distribution between wells. **d** The 3D regional permeability model established with spherical type. **e** The 3D fence diagram of D for well group B6–3~B1~B4–3~B7~B3–2~B3–6. **f** Connecting-well section of permeability model of B8~B4~B7~B7–5~B15–2, showing the horizontal and vertical permeability distribution between wells in each layer

If plane distributive and expanding characteristics proved well by comprehensive judgment between prophase geological research results and simulated property model, it indicates that the simulated property model has high precision. The average porosity and permeability of the study area are 18 % and 45×10^{-3} μm², respectively. It can be seen from the histogram of property probability distribution that the average porosity and permeability from property model were 19 % and 48×10^{-3} μm², which accords with the actual physical properties.

(2) Comparison between facies-controlled model and nonfacies-controlled model

Geological models are established based on random function theory which can generate a series of equal probability stochastic simulation model. Because geologic parameter has a certain randomness and the generated random model also has a great deal of uncertainty, there exists difference with the actual geological conditions and thus not conducive to make accurate characterization of the reservoir. Through the comparison between the facies-controlled and nonfacies-controlled models, the result shows that facies-controlled model has higher accordance with the actual geological situation.

(3) Make calibration with dynamic data

Sedimentary facies can reflect the distribution and connectivity of sand bodies, by checking whether there exist close contact between pressure change and injection-production relation of production well. Therefore, in the actual research, we can take advantage of highly reliable and meaningful dynamic data to validate the model (Sun et al. 2010).

Conclusions

The main target of the paper was to establish the 3D reservoir model of the third oil set of the second member of Funing Formation ($E_1f_2^3$) at regional scale from random interpolation process originally for geological research. All the presented research results may reasonably lead to the following conclusions:

(1) Through weighting, different sedimentary facies zones can be given different focus on reservoir variations, and hence changes the bandwidth and the search scope of sequential search, allowing grid cells to be retained or grouped differently. The spatial variability of the modeled microfacies is taken into account through repeating adjustment of variograms in major, minor, and vertical directions based on regression analysis between the length and width of facies belt. The result shows that the simulated facies model can provide reliable guidance for quantifying reservoir parameters.

(2) Although there are nine types of logging discretization method, they are not all suitable for the study area. After comparison through observing the results of the logging data before and after processing, maximum algorithm is suitable for discretization in BD oilfield.

(3) The study area is a fractured sandstone reservoir, possessing characteristics of low permeability, well-developed facture, and strong reservoir heterogeneity;

thus, reservoir parameters vary accordingly in a certain range in different sedimentary facies belt. Sequential indicator simulation which is more conducive to display reservoir heterogeneity is used combined with facies-controlled modeling. And, assigned value simulation is used to construct mudstone model. By comparison between distribution characteristics of each sedimentary facies and its corresponding physical property, it was found that reservoir property in sandbar zones is better than that in sandbeach zones.

References

Al Bulushi NI, King PR, Blunt MJ, Kraaijveld M (2012) Artificial neural networks workflow and its application in the petroleum industry. Neural Comput Appl 21(3):409–421

Archer J.S., C.G. Wall. Petroleum engineering principles and practice [M].1992: 140–153

Bhatt A, Helle HB (2002) Determination of facies from well logs using modular neural networks [J]. Pet Geosci 8:217–228

Chen Y, Durlofsky LJ (2006) Adaptive local–global upscaling for general flow scenarios in heterogeneous formations. Transp Porous Media 62:157–185

Deutsch CV (2002) Geostatistical reservoir modeling [M. Oxford University Press, New York

Durlofsky LJ, Jones RC, Milliken WJ (1997) A nonuniform coarsening approach for the scale up of displacement processes in heterogeneous media. Adv Water Resour 20:335–347

Fegh A, Riahi MA, Norouzi GH (2013) Permeability prediction and construction of 3D geological model: application of neural networks and stochastic approaches in an Iranian gas reservoir [J]. Neural Comput Applic 23:1763–1770

Haykin S (1999) Neural networks: a comprehensive foundation [M]. Prentice Hall, London, pp. 20–25

Isaaks EH, Srivastava RM (1989) An introduction to applied geostatistics [M. Oxford University Press, New York

James W, Jennings JR, Jerry LF (2003) Predicting permeability from well logs in carbonates with a link to geology for inter-well permeability mapping. SPE Reserv Eval Eng 6(4):215–225

Kulpecz AA, van Geuns LC (1990) Geological modeling of a turbidite reservoir, Fortier field, North Sea. Sandstone Petroleum Reservoirs: 489–507

Laine E (2014) Geological 3D modeling (process) and future needs for 3D data and model storage at geological survey of Finland. Mathematics of Planet Earth 839-842

Mao F, An'ding C, Yuanfeng Y et al (2006) Hydrocarbon accumulation characteristics and seismic recognition technology of complex small fault block in northern Jiangsu basin [J]. Oil Gas Geol 27(6):828

Monsen E, Randen T, Sønnelan L (2005) Geological model building: a hierarchical segementation approach [J]. Math Methods Model Hydrocarb Explor Prod 7:213–245

Seifert D, Jensen JL (1999) Using sequential indicator simulation as a tool in reservoir description: issues and uncertainties. Math Geol 31(5): 527–550

Sun L, Liu J, Mao J et al (2010) The application of injection profile data in the low permeability reservoir development [J]. Petrochem Ind Appl 29(12):44–46

Tao J, Xu L, Huang J, Yu B Research on the prediction of the geological spatial information using gray GIS modeling method based on the borehole data and the geologic map [J]. Geo-Informatics in Resource Management and Sustainable Ecosystem 399:107–115

Tureyen OI, Caers J (2005) A parallel, multiscale approach to reservoir modeling. Comput Geosci 9:75–98

Turner AK (1989) The role of three dimensional geographic information systems in subsurface characterization for hydrogeological applications. In: Raper JF (ed) Three-dimensional applications in geographic information systems. Taylor and Francis, London, pp. 115–127

Turner AK (2000) Geoscientific modelling: past, present and future. In: Coburn TC, Yarus JM (eds) geographic information systems in petroleum exploration and development. AAPG computer applications in geology. American Association Petroleum Geologists 4:27–36

Turner AK (2006) Challenges and trends for geological modelling and visualization [J]. Bull Eng Geol Env 65:109–127

Wang Y, Liu B, Gao J, Zhang X, Li S, Liu J, Tian Z (2015) Auto recognition of carbonate microfacies based on an improved back propagation neural network [J]. J Cent South Univ 22:3521–3535

Wenlong X., Tran T., Srivastava R.M., Journel A.G.. Integrating seismic data in reservoir modeling: The Collocated Cokriging Alternative. In: the 67th annual technical conference and exhibition of the society of petroleum engineers, Washington, 1992, 4–7.

Yeten B, Gumrah F (2000) The use of fractal geostatistics and artificial neural networks for carbonate reservoir characterization. Transp Porous Media 41:173–195

Zhang Q, Xu S, Yu W, Cheng H (2011) Application of particle swarm optimization to kriging three dimensional geological modeling. Journal of Daqing Petroleum Institute 35(1):85–89

Zhao C, Zhu X (2001) Sedimentary petrology[M]. Petroleum Industry Press, Beijing

Zheng G, Shen Y (2004) 3D analyses of geological characteristics and status research of 3D geology modeling. Adv Earth Sci 19(2):218–223